

Modulation of diarylethene fluorescence by photochromic switching and solvent polarity

Sofia K. Lazareva, Evgeni M. Glebov, Anatoly V. Metelitsa, Andrey G. Lvov, Valerii Z. Shirinian, Marianna Gregova-Trencanova, Dushan Velic and Artem B. Smolentsev

Table of contents

I. General information	2
II. Spectral properties in different solvents	3
III. Energy profile for DCP1	5
IV. Luminescence decay of DCP1 in different solvents	6
V. Temporal profiles of DCP1 photostimulated emission	7
VI. Visible light switching of DCP1	8
VII. References	9

I. General information

I-a. Experimental details

Synthesis and physical properties of **DCP1** were reported elsewhere.¹ Spectrophotometric grade solvents (Panreac) were used without additional purification. UV absorption spectra were recorded using Varian Cary 50 spectrophotometer. Stationary luminescence spectra were recorded on a Hitachi MPF-4 and Cary Eclipse spectrofluorimeters. Emission quantum yields ϕ_f were determined using quinine bisulfate in 0.5 M H₂SO₄ as a reference.² Nanosecond luminescence was recorded using the FLSP-920 spectrofluorimeter (Edinburgh Instruments). A high pressure mercury lamp with a set of glass filters (313 nm) as well as LEDs (400 and 530 nm) were used for irradiation. Quantum yields of photochromic transformations A \leftrightarrow B (Scheme 1) $\phi_{A\rightarrow B}$ and $\phi_{B\rightarrow A}$ as well as closed (B) form molar absorption coefficient ϵ_B were determined by kinetic method described previously.^{3,4} Power meter SOLO 2 (Gentec) was used to measure the radiation intensity for the quantum yield calculations.

Ultrafast time-resolved fluorescence was studied by means of up-conversion technique. A mode-locked Ti-sapphire oscillator (CDP) was pumped with a continuous-wave laser (Verdi, Coherent) with an output wavelength of 800 nm, a pulse of 100 fs, a width spectrally broadened to 20 nm, and an output power of 300 - 450 mW, pulse repetition rate 86 MHz. The fundamental pulse of 800 nm was converted to 400 nm and this wavelength was used to excite the sample within the time-resolved fluorescence up-conversion spectrometer FOG 100 (CDP).

I-b. Lippert-Mataga plot

The assumption that the **DCP 1** fluorescence is emitted from the ICT state was supported by the Lippert-Mataga plot (Fig. S1), which is the dependence of the Stokes shift on the solvent polarity.⁵ It allows one to estimate the dipole moment increase in the excited state. The dependence is expressed as followed:

$$\Delta\tilde{\nu} = \tilde{\nu}_{abs} - \tilde{\nu}_{fl} = \frac{2(\mu_e - \mu_g)}{hca^3} \Delta f + const \quad (1)$$

$$\Delta f = \frac{\epsilon_d - 1}{2\epsilon_d + 1} - \frac{n^2 - 1}{2n^2 + 1} \quad (2)$$

where $\tilde{\nu}_{abs}$ and $\tilde{\nu}_{fl}$ are the wavenumbers of the absorption and fluorescence maxima; $\Delta\tilde{\nu}$ denoted the Stokes shift; μ_g and μ_e are ground and excited states dipole moments respectively; ϵ_B and n are the dielectric constant and refractive index of the medium; h is Planck's constant, c is the velocity of light and a is the radius of the solvent cavity in which the fluorophore resides (Onsager cavity radius). The Onsager cavity radius of 5.86 Å was calculated by DFT method using the Gaussian 09 program package.⁶ The Gaussian matrix "freq b3lyp/6-31g volume" was used. The function Δf is called the orientation polarizability, it accounts for the spectral shifts due to reorientation of the solvent molecules.

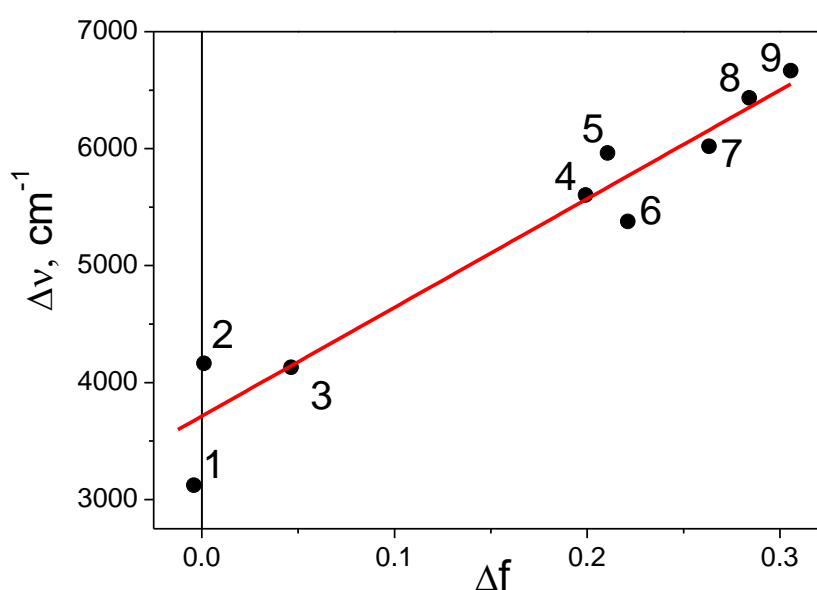
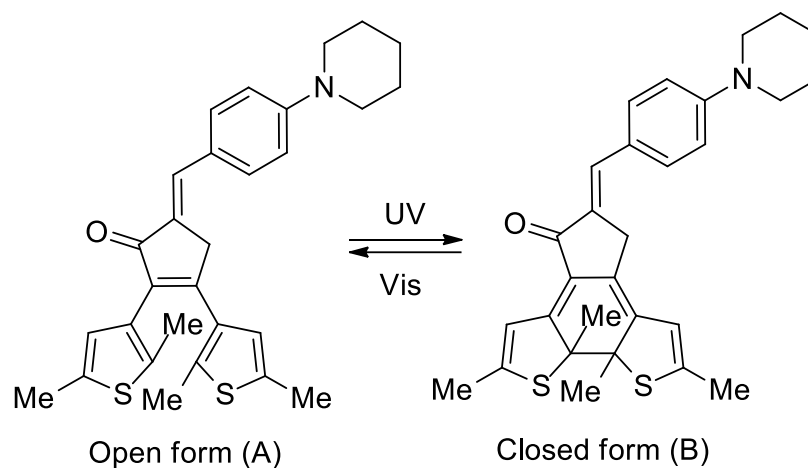


Figure S1. Lippert-Mataga plot for **DCPI**. The solvents are numbered according to the Table S1). The straight line represents the best least-square fit to the data.

II. Spectral properties in different solvents

Table S1. Spectral characteristics of **DCP1** in different solvents. ϵ_d – dielectric constant; n – refractive index of the solvent; λ_{Amax} – absorbance band maxima; λ_{Fmax} – fluorescence band maxima; $\Delta\nu$ - Stokes shift.



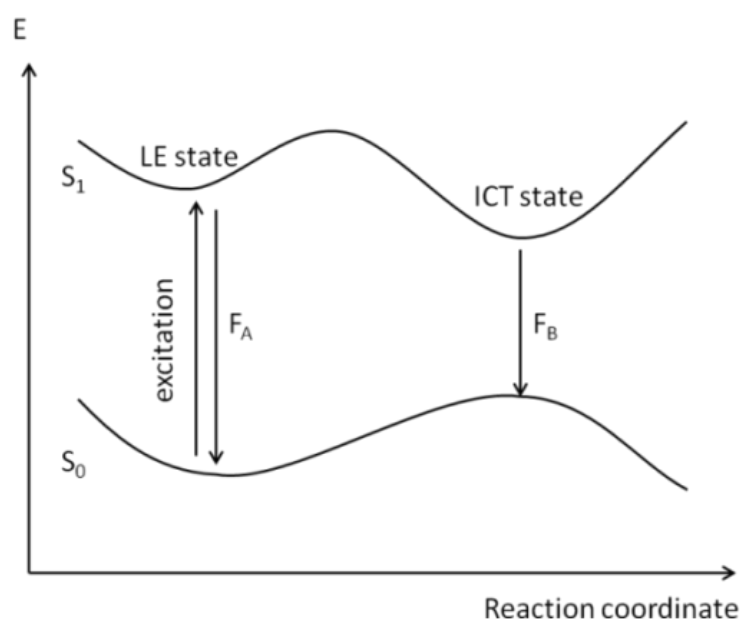
№	Solvent	ϵ_d	n	$\lambda_{Amax}, \text{nm}$	$\lambda_{Fmax}, \text{nm}$	$\Delta\nu, \text{cm}^{-1}$
1	n-hexane	1.9	1.3751	379	450	4163
2	cyclohexane	2.0	1.4263	383	435	3121
3	toluene	2.8	1.4969	395	472	4130
4	ethyl acetate	6.0	1.3726	393	504	5604
5	tetrahydrofuran	7.6	1.405	394	515	5963
6	1,2-dichloroethane	10.4	1.4448	407	521	5376
7	acetone	20.7	1.3591	398	535	6434
8	acetonitrile	38	1.3442	403	551	6665
9	DMSO	45	1.477	416	555	6020

Table S2. Photochromic and fluorescent characteristics of **DCP1**. ϵ_d – dielectric constant; λ_{Amax} – absorbance band maxima; ϵ_{max}^A – molar absorption coefficient at absorbance band maxim; λ_{Fmax} – fluorescence band maxima; ϕ_F – fluorescence quantum yield (excitation at 313 nm); $\phi_{A\rightarrow B}$ – photocyclization quantum yield (irradiation at 313 nm); $\phi_{B\rightarrow A}$ – ring-opening reaction quantum yield (irradiation at 530 nm); ϵ_{max}^B – molar absorption coefficient of B form at 530 nm; F_{PSS}/F_0 - ratio of fluorescence intensities of the photostationary state and the solution before irradiation.

Solvent	ϵ_d	λ_{Amax} , nm	$\epsilon_{max}^A \times 10^{-4}$, $M^{-1}cm^{-1}$	λ_{Fmax} , nm	ϕ_F	$\phi_{A\rightarrow B}$	$\phi_{B\rightarrow A}$	ϵ_{max}^B , $M^{-1}cm^{-1}$	F_{PSS}/F_0
n-hexane	1.8	379	2.9	450	0.002	0.1	0.05	10000	0.30
toluene	2.8	395	2.6	472	0.03	0.08	0.05	10500	0.15
1,2-dichloroethane	10.4	407	2.7	521	0.14	0.05	0.03	8300	0.25
DMSO	45	416	2.3	555	0.19		0.02	12000	0.48

III. Energy profile for DCP1

Figure S2. Tentative scheme of energy profile for compounds with the dual luminescence. LE – locally excited state, ICT – intramolecular charge transfer state, F_A , F_B – fluorescence from the corresponding states.



IV. Luminescence decay of DCP1 in different solvents

Figure S3. Kinetics of DCP1 luminescence decay in 1,2-dichloroethane. Excitation at 375 nm, 1 cm cell, absorbance at excitation wavelength 0.2. Red curve – experiment, black curve – IRF, green curve – 1-exponential fit.

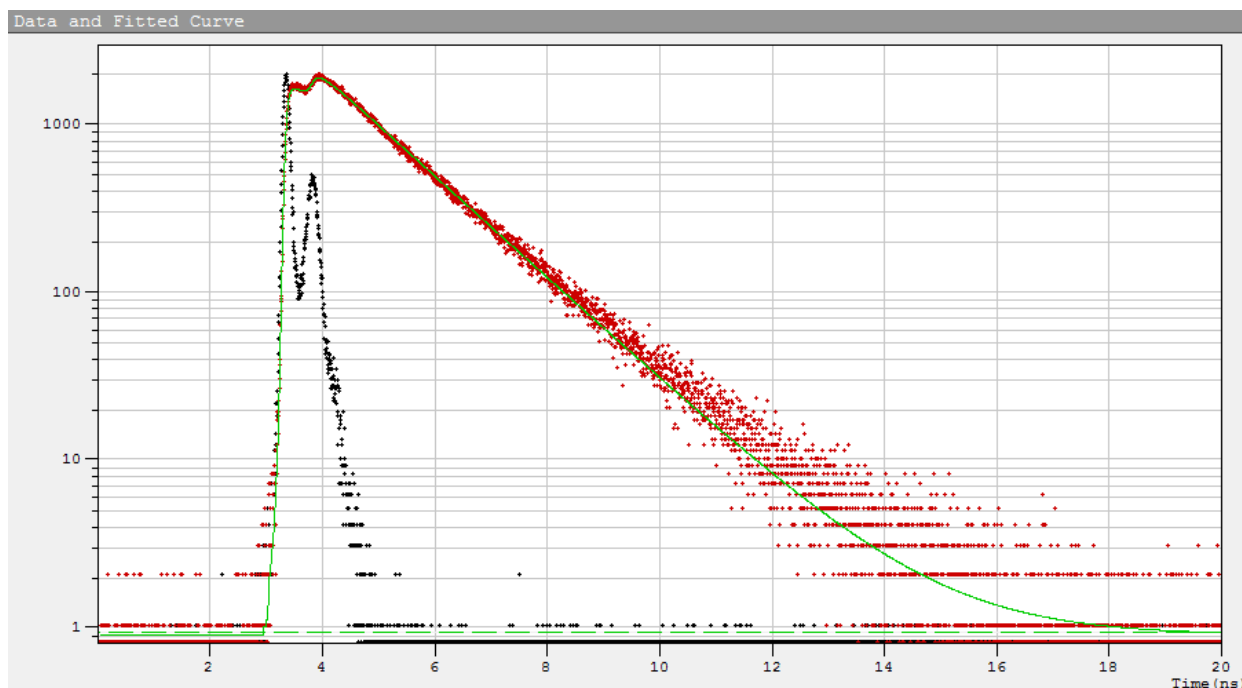


Figure S4. Kinetics of DCP1 luminescence decay in toluene. Excitation at 375 nm, 1 cm cell, absorbance at excitation wavelength 0.2. Red curve – experiment, black curve – IRF, green curve – 1-exponential fit.

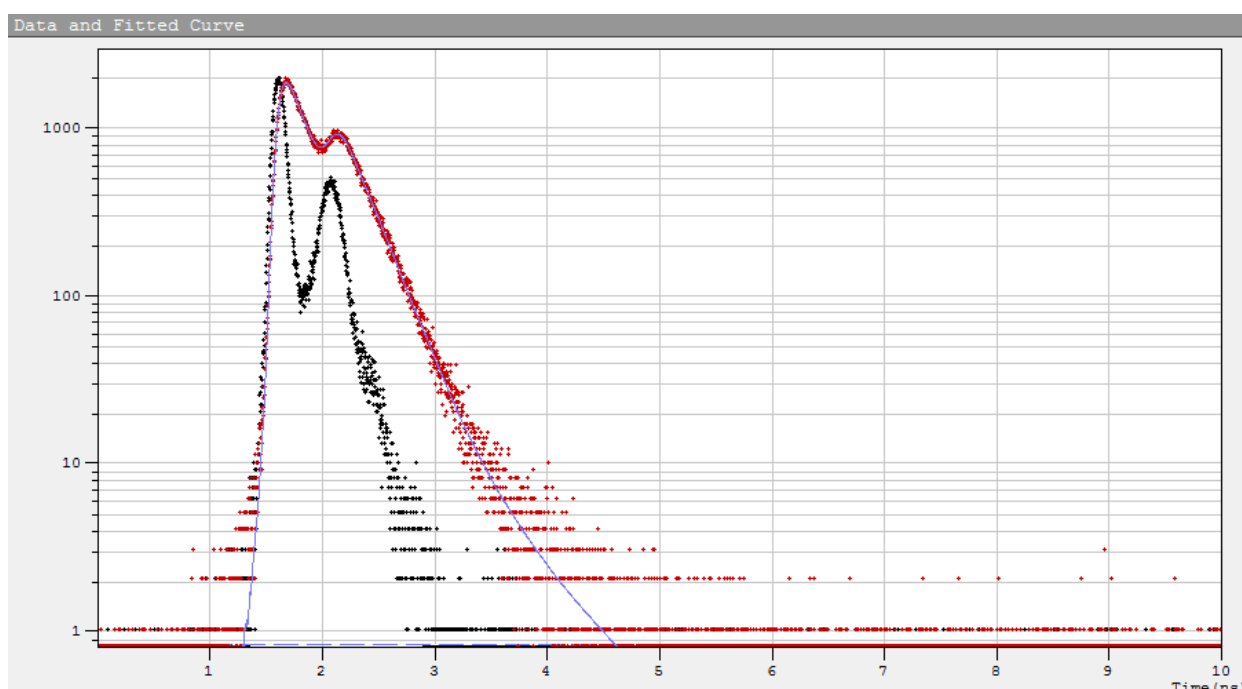
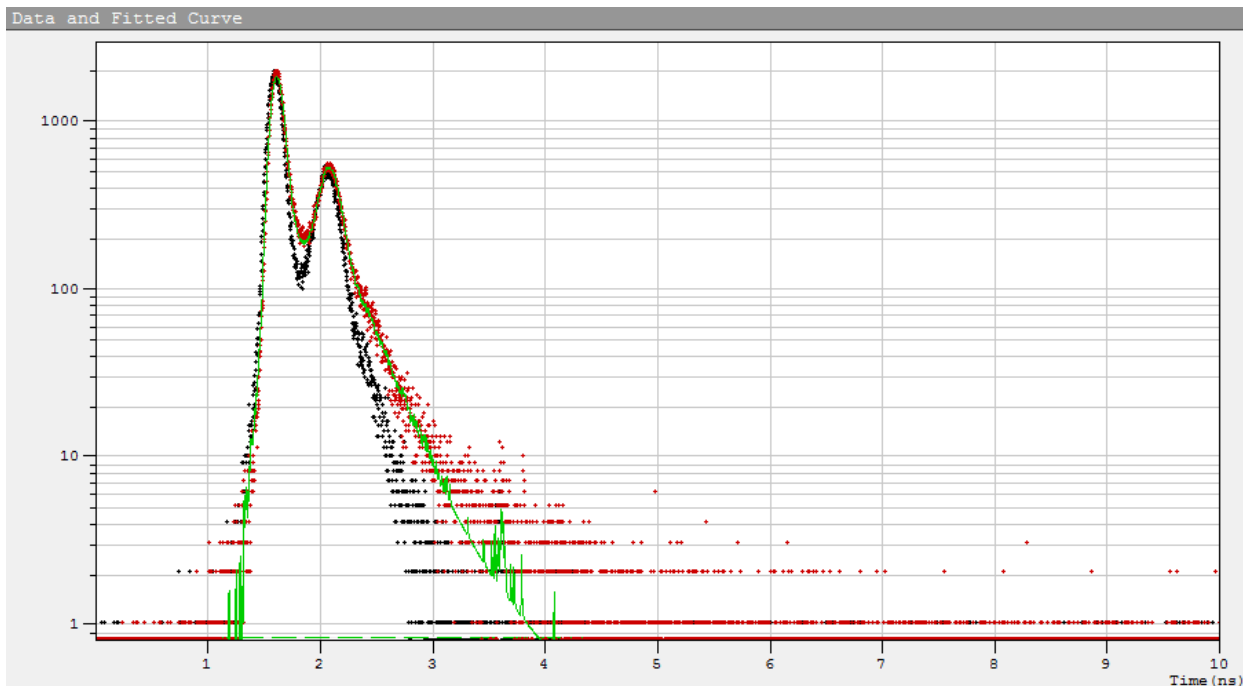
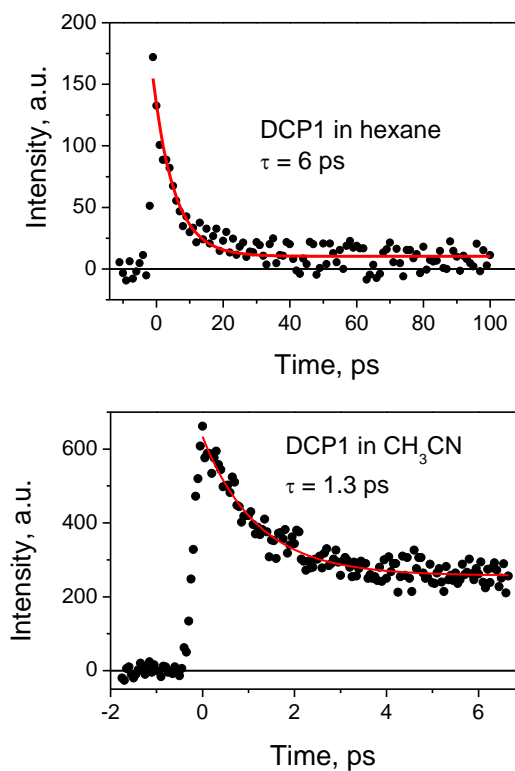


Figure S5. Kinetics of DCP1 luminescence decay in hexane. Excitation at 375 nm, 1 cm cell, absorbance at excitation wavelength 0.2. Red curve – experiment, black curve – IRF, green curve – 1-exponential fit.



V. Temporal profiles of DCP1 photostimulated emission

Figure S6. Temporal profiles of DCP1 photostimulated emission at 400 nm (excitation at 400 nm) in hexane (top) and acetonitrile (bottom) along with the monoexponential fit functions (red lines).



VI. Visible light switching of DCP1

In these experiments, visible light irradiation was performed by blue and green LED sources (100 x 0.1 W).

Scheme S1. Switching of **DCP1** by visible light.

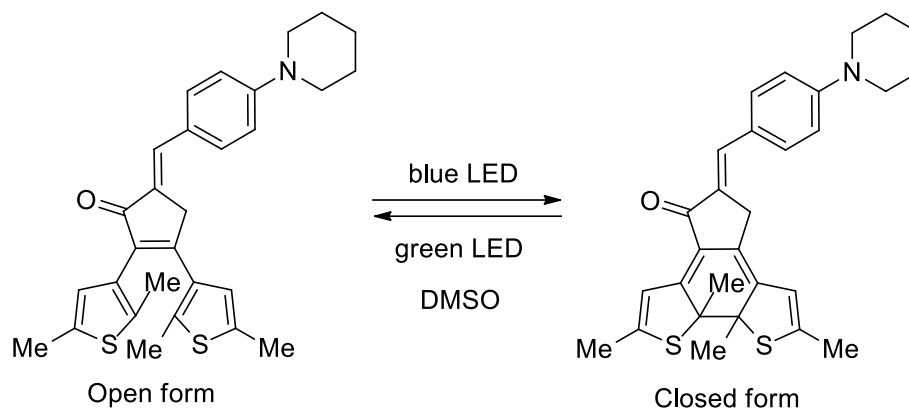


Figure S7. Electronic absorption spectra of **DCP 1** in DMSO (2.1×10^{-5} M) before and after irradiation with blue and green LED light sources.

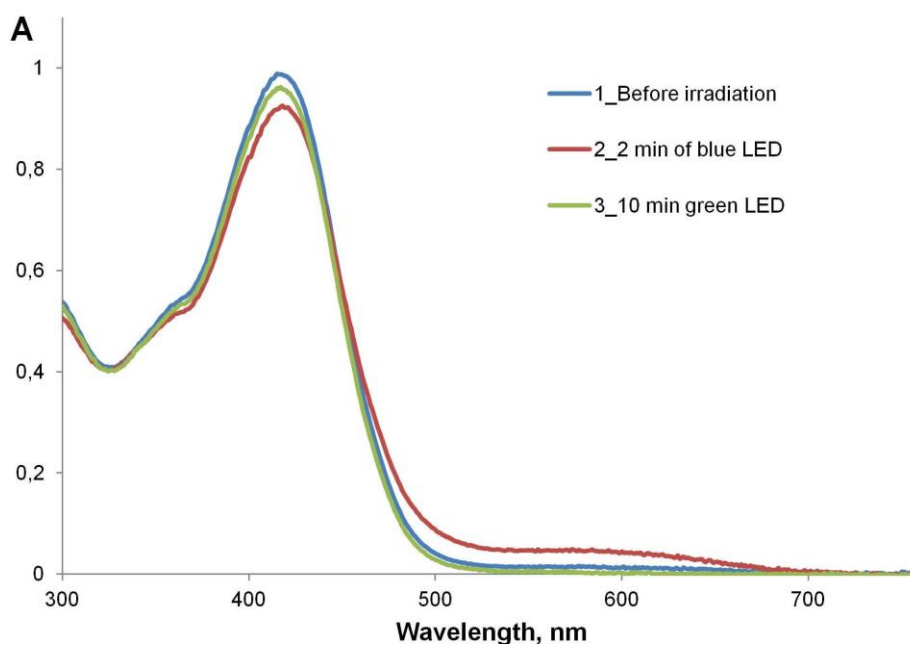
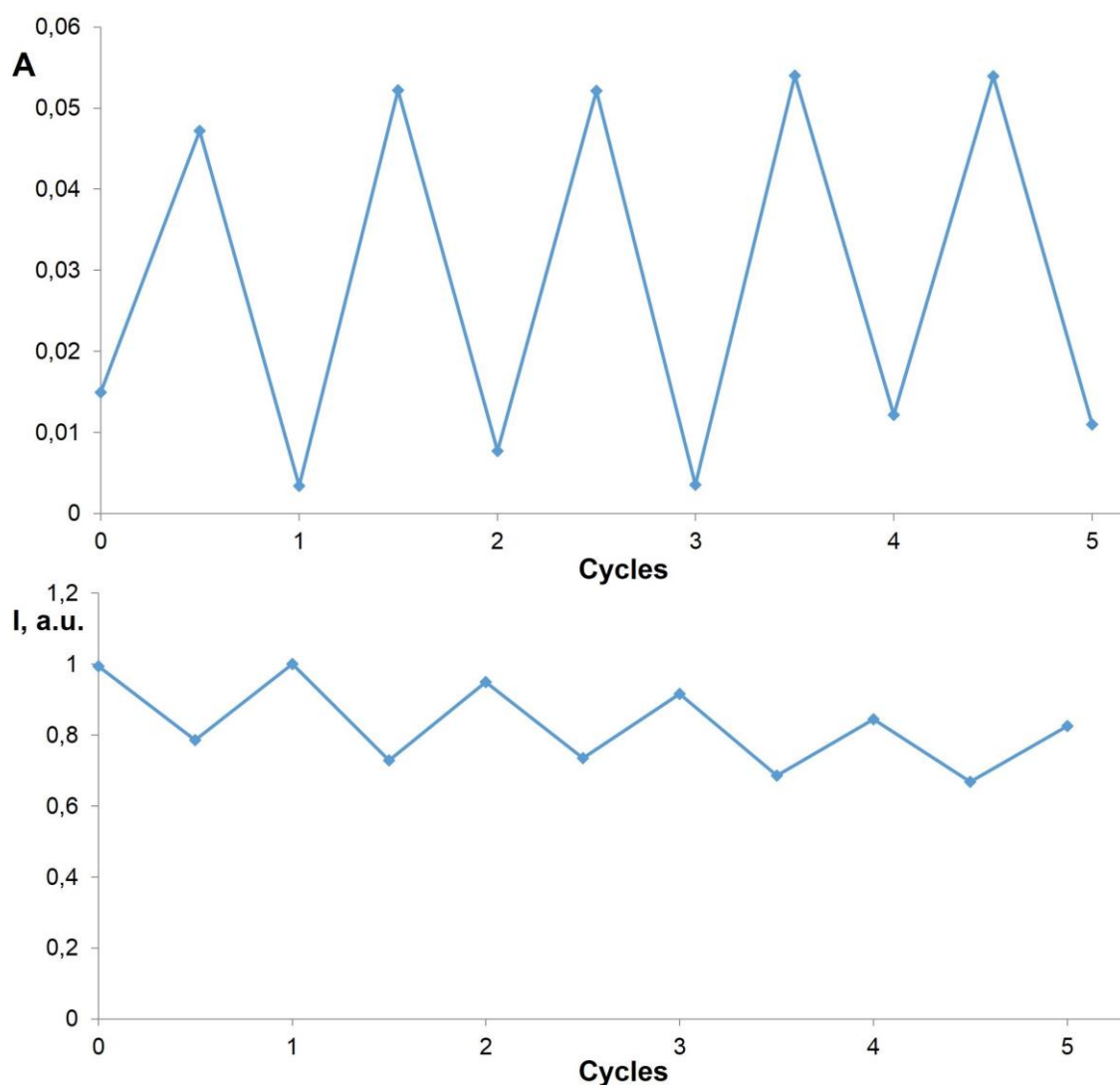


Figure S8. Photoswitching of **DCP 1** in DMSO. Absorption at 555 nm (upper panel) and fluorescence intensity (lower panel; $\lambda^{\text{ex}} = 365 \text{ nm}$, $\lambda^{\text{em}} = 555 \text{ nm}$) by subsequent irradiation with blue (2 min) and green (10 min) LED light.



VII. References

- ¹ V.Z. Shirinian, A.A. Shimkin, D.V. Lonshakov, A.G. Lvov and M.M. Krayushkin, *J. Photochem. Photobiol. A: Chem.*, 2012, **233**, 1.
- ² D.F. Eaton, *Pure Appl. Chem.*, 1988, **60**, 1107.
- ³ M. Cipolloni, F. Ortica, L. Bougdid, C. Moustrou, U. Mazzucato and G. Favaro, *J. Phys. Chem. A*, 2008, **112**, 4765.
- ⁴ V.V. Semionova, E.M. Glebov, A.B. Smolentsev, V.V. Korolev, V.P. Grivin, F. Plyusnin and V.Z. Shirinian, *Kinet. Catal.*, 2015, **56**, 318.
- ⁵ P.A. Panchenko, A.N. Arkhipova, O.A. Fedorova, Yu. V. Fedorov, M.A. Zakharko, D.E. Arkhipov and G. Jonusauskas, *Phys. Chem. Chem. Phys.*, 2017, **19**, 1244.

⁶ M.J. Frisch, G.W. Trucks, H.B. Schlegel, G.E. Scuseria, M.A. Robb, J.R. Cheeseman, G. Scalmani, V. Barone, B. Mennucci, G.A. Petersson, H. Nakatsuji, M. Caricato, X. Li, H.P. Hratchian, A.F. Izmaylov, J. Bloino, G. Zheng, J.L. Sonnenberg, M. Hada, M. Ehara, K. Toyota, R. Fukuda, J. Hasegawa, M. Ishida, T. Nakajima, Y. Honda, O. Kitao, H. Nakai, T. Vreven, J.A. Montgomery, Jr., J.E. Peralta, F. Ogliaro, M. Bearpark, J.J. Heyd, E. Brothers, K.N. Kudin, V.N. Staroverov, R. Kobayashi, J. Normand, K. Raghavachari, A. Rendell, J.C. Burant, S.S. Iyengar, J. Tomasi, M. Cossi, N. Rega, J. M. Millam, M. Klene, J.E. Knox, J.B. Cross, V. Bakken, C. Adamo, J. Jaramillo, R. Gomperts, R.E. Stratmann, O. Yazyev, A.J. Austin, R. Cammi, C. Pomelli, J.W. Ochterski, R.L. Martin, K. Morokuma, V.G. Zakrzewski, G.A. Voth, P. Salvador, J.J. Dannenberg, S. Dapprich, A.D. Daniels, Ö. Farkas, J.B. Foresman, J.V. Ortiz, J. Cioslowski and D.J. Fox, *Gaussian 09* (Gaussian, Inc., Wallingford CT, 2009).